Citation: Partridge, J, Field, M, Peng, J, Sadek, A, Kalantar-Zadeh, K, Du Plessis, J and McCulloch, D 2008, 'Nanostructured SnO2 films prepared from evaporated Sn and their application as gas sensors', Nanotechnology, vol. 19, no. 12, pp. 1-5.

Nanostructured SnO_2 films prepared from evaporated Sn and their application as gas sensors

J G Partridge[1], M R Field[1], J L Peng[1], A Z Sadek[2], K Kalantar-zadeh[2], J Du Plessis[1] and D G McCulloch[1,3]

[1] Applied Physics, School of Applied Sciences, RMIT University, Melbourne, Victoria 3001, Australia

[2] School of Electrical and Computer Engineering, RMIT University, Melbourne, Victoria 3001, Australia

[3] Email: dougal.mcculloch@rmit.edu.au

Abstract

This paper describes the morphology, stoichiometry, microstructure and gas sensing properties of nano clustered SnO_x thin films prepared by Sn evaporation followed by the Rheotaxial Growth and Thermal Oxidation (RGTO) process. Electron microscopy was used to investigate, in detail, the evolution of the films as the oxidation temperature was increased. The results showed that the contact angle, perpendicular height, volume and microstructure of the clusters all changed significantly as a result of the thermal oxidation processes. Electron diffraction and X-ray photoelectron spectroscopy measurements revealed that after oxidation at a temperature of 600 ºC, the Sn clusters were fully transformed into porous 3-dimensional polycrystalline SnO_2 clusters. Based on these results, a prototype SnO_2 sensor was fabricated and sensing measurements were performed with H_2 and NO_2 gases. At operating temperatures of 150 ºC - 200 ºC the film produced measurable responses to concentrations of H_2 as low as 600 ppm and NO_2 as low as 500 ppb.

PACS CODES: 07.07.Df (Sensors), 36.40.-c (Atomic and molecular clusters), 81.07.-b (Nanoscale materials and structures: fabrication and characterization).

1. Introduction

SnO_2 is a semiconducting metal oxide which has received a great deal of attention from researchers and industry alike. This is largely due to its gas sensing capability (see for example [1]). Nano-structured SnO_2 films have been produced by various research groups as their surface to volume ratio is large and they offer potentially higher sensitivity as a result (see for example [2,3,4]). With careful process control, the size of the grains within the films can be made comparable to the depth of the space-charge layer formed within each grain, thereby further improving sensitivity. However, the relationship between the electrical and nano-structural properties of sensing films has not yet been fully established [3].

The list of applications for SnO_2 does not end with sensors. Undoped and doped transparent conducting SnO_2 films have been studied extensively because they can exhibit high optical transmission and electrical conduction [5]. Recently, lightly Ta-doped SnO_2 nanowires were also used to produce fully transparent FET type devices [6]. The increasing number of applications for this material provides further motivation for investigating the structure of films, clusters and nanowires and relating the findings to electrical, optical and mechanical properties.

Deposition methods employed to produce SnO_2 films include pulsed laser deposition [7], evaporation [8] and sputtering [9]. SnO_2 films can also be readily produced from Sn films followed by thermal oxidation. The latter approach is potentially useful for gas sensing applications because Sn films tend to grow on oxide surfaces in the Volmer Weber mode (ie. as islands or clusters) and with high area-to-volume ratios. The rheotaxial growth and thermal oxidation (RGTO) process was developed with the aim of retaining the morphology of the original Sn film after conversion to SnO_2 [10]. Stage one of the process involves heating the Sn sample (in the presence of oxygen) to a temperature just below the melting point of Sn (typically about 200 ºC) in order to increase the thickness of the native oxide layer. This thickened oxide shell

supports the Sn core and resists deformation during a subsequent higher temperature process (typically 600 ºC - 700 ºC) which transforms the remaining Sn into SnO_2. The RGTO method has been used by various research groups and has proved effective for complete oxidation of films, and nanowires [8,11]. Despite its widespread use, a detailed microstructural investigation of the evolution of Sn films into SnO_2 using the RGTO process has not yet been performed.

Previous studies on SnO_2 thin films produced by thermal oxidation of Sn thin films have been reported [12,13,14] and these papers have described the phase transformations which occur during thermal oxidation at various temperatures. However, despite their suitability for sensing applications, a detailed Transmission Electron Microscopy (TEM) study of the nanostructure of thermally oxidised SnO_2 cluster/island films is absent from the literature. In this paper, we employ X-ray photoelectron spectroscopy and electron microscopy to investigate the stoichiometry, microstructure and morphology of evaporated Sn cluster films following RGTO processing to different maximum temperatures. Plane view and cross-sectional TEM have been used to provide a detailed view of the microstructure of thermally oxidised SnO_2 films. Finally, based on these results, a prototype RGTO processed SnO_2 sensor was fabricated and its sensitivity to NO_2 and H_2 was investigated.

2. Experiment

2.1. Sample preparation

P-type Si substrates with a 1 μm thickness layer of SiO_2 were selected to support the Sn and SnO_x films. Four samples were prepared in a single deposition process. Sn (99.99% purity pellet) was thermally evaporated from a tungsten filament boat inside a DynaVac coating system to produce a film with a nominal deposited thickness of 40 nm on each of the four SiO_2 covered Si substrates. The deposition rate was approximately 0.2 nm/s and the base pressure and process pressure were 1×10^{-6} Torr and 5×10^{-6}

Torr, respectively. After the deposition, these samples were processed individually as follows; Sample '*AsDep*' was the as-deposited sample, sample '*Ox200*' was heated to 200 ºC, sample '*Ox400*' was heated to 200 ºC then 400 ºC and sample '*Ox600*' was heated to 200 ºC, 400 ºC and finally 600 ºC. Samples were held at each temperature (200 ºC, 400 ºC and 600 ºC) for 2-hours and the ramp time between these temperatures was approximately 30 minutes. The samples were all heated in air at atmospheric pressure using a simple bench-top furnace. Samples with coverage approximately equal to the percolation threshold were prepared so that individual clusters could be counted and measured reliably from Scanning Electron Microscopy (SEM) images. Adopting this coverage also enabled images of individual cross-sectioned clusters to be produced by TEM.

The contacted substrate required for the gas sensing measurements was fabricated using a photo-plot mask and optical lithography. The total length of each interdigital-type contact was approximately 35 mm and the contact-to-contact separation was approximately 100 μm. A prototype sensor with a SnO_2 film of 80 % area coverage (ie. just above the percolation threshold) was produced initially but its resistance was too high for reliable sensing measurements. An evaporation-RGTO-evaporation-RGTO process sequence was then used to produce a device with a thicker porous SnO_2 film. This had a resistance at 200 ºC in air of approximately 8 kΩ. Alternating evaporations and RGTO processes have previously been employed to produce 'stacked' SnO_2 cluster films with high surface area and reduced film resistance [15]. A nominal thickness of 40 nm was deposited in each of the two evaporations and the temperature sequence for the thermal oxidation was identical to that used for the *Ox600* sample; 200 ºC (2-hrs), then 400 ºC (2-hrs) and finally 600 ºC (2-hrs) with 30-min ramp times between each set-point temperature. Once complete, the sample was placed in a multi-channel gas calibration system and the contact-to-contact resistance was measured during timed exposures to various concentrations of NO_2 gas.

2.2. Electron Microscopy and X-ray Photoelectron Spectroscopy

SEM imaging of the samples was performed using a FEI-Nova NanoSEM and image processing software enabled particle counts and particle areas to be calculated from the captured images. TEM specimens were prepared either in plane view or cross-section by mechanical polishing using a tripod polisher, followed by Ar ion beam thinning to electron transparency. They were analysed in a JEOL 2010 Transmission Electron Microscope operating at 200 kV.

X-ray Photoelectron Spectroscopy (XPS) was performed on a VG Microlab 310F with a dual Al/Mg anode unmonochromated X-ray source operated at a power of 300 W and with a 15 kV excitation voltage. The sample was tilted such that the electron analyzer normal to the sample surface collected the escaping electrons. The analyzed area is determined by the electrostatic lens and slits of the analyzer and in this case the rectangular area was approximately 5×1 mm^2. A SnO_2 powder standard [16] was used to calibrate the sensitivity factors prior to the measurements and the samples were sputtered in-situ with Ar gas (at a pressure of 0.2 μTorr) in order to purge the surface of carbon contaminants.

3. Results and Discussion

3.1. SnO_2 cluster film morphology and area distribution

Figure 1 shows the surface morphology of the evaporated Sn/SnO_x films. Fig. 1(a) shows sample *AsDep* (with no RGTO treatment) whilst Fig. 1(b) shows the *Ox400* sample and Fig. 1(c) shows the *Ox600* sample. The corresponding area distributions obtained from the images in Fig. 1 are shown in Fig. 2. The as-deposited film has grown in Volmer-Weber mode and consists of islands (clusters) with an average area of 4000 nm^2. In addition to large islands, there is a population of small islands with areas of less than 2000 nm^2. It can be seen from Fig. 2 that following oxidation at 600 ºC, there is a tendency for the average island area to increase (from 4000 nm^2 to 5500 nm^2). This increase in the area of the islands can be attributed to coalescence of neighbouring islands and Ostwald ripening [17]. The population of small islands that

remained following annealing suggested that these islands were less mobile and therefore less able to coalesce with their neighbours.

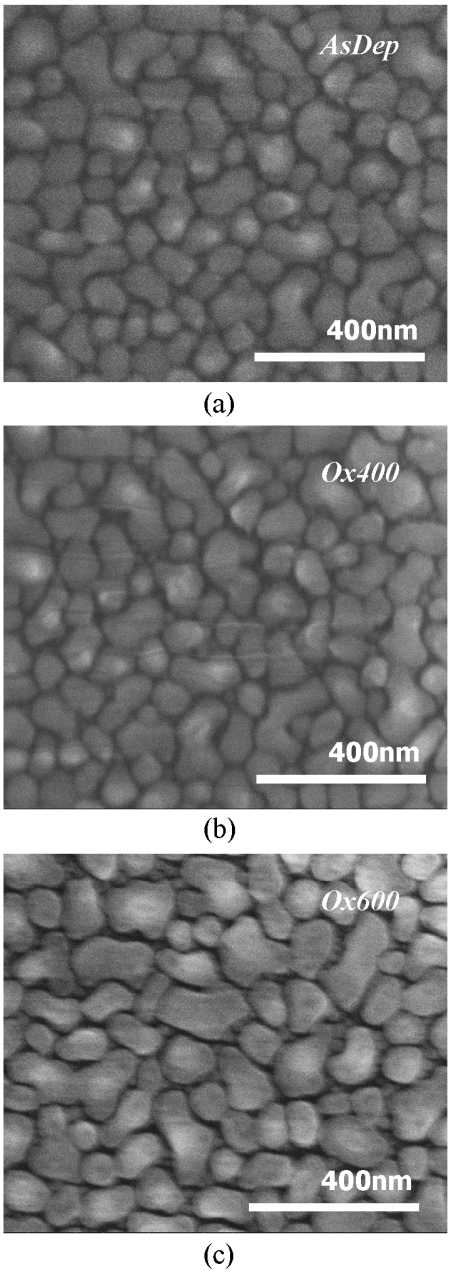

Figure 1. SEM images of evaporated Sn cluster films (a) as deposited, (b) after oxidation at temperatures of 200 ºC and 400 ºC and (c) after oxidation at temperatures of 200 ºC, 400 ºC and 600 ºC.

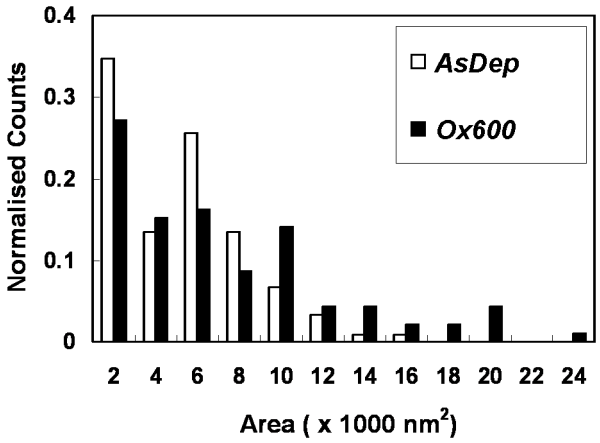

Figure 2. Cluster area distributions within thermally evaporated Sn films as deposited (sample-*AsDep*) and after oxidation at temperatures of 200 ºC, 400 ºC and 600 ºC (sample-*Ox600*).

3.2. XPS measurement of stoichiometry

X-ray Photoelectron Spectroscopy (XPS) spectra in the vicinity of the Sn 3d peaks from the as-deposited and *Ox600* samples are shown in Fig. 3. The Sn 3d5 spectrum from the as-deposited sample has a main peak at approximately 487 eV which corresponds to a mixture of predominantly SnO_2 and other oxidation states as well as a shoulder at approximately 485 eV which corresponds to metallic Sn [18]. This indicates that the islands on the as-deposited film are partially oxidised. Following annealing only peaks from SnO_2 are observed [18] and this stoichiometry was confirmed using peak area analysis. It is important to note that XPS can only probe the near surface region of a sample so the composition of the various samples was also investigated using selected area diffraction analysis (see below).

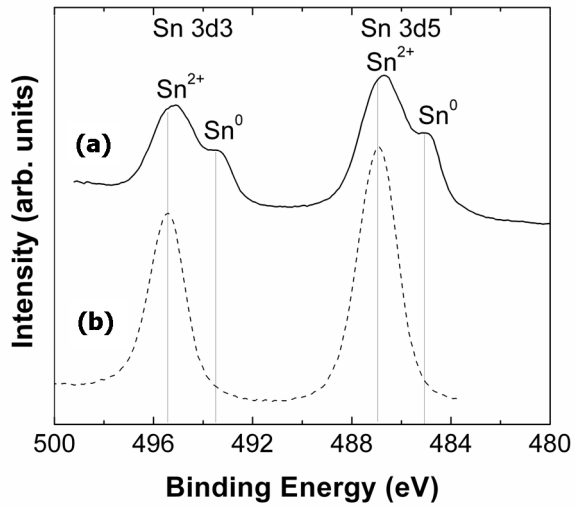

Figure 3. XPS spectra for evaporated Sn (a) as-deposited and (b) after oxidation at temperatures of 200 ºC, 400 ºC and 600ºC.

3.3. TEM characterization of SnO_2 cluster films

Plan view TEM images of the as-deposited and the sample *Ox600* are shown in Fig. 4. The *AsDep* sample (Fig. 4(a)) contained irregular shaped islands from 5 nm to 100 nm in length and with heights less than 30 nm. A thin surface oxide shell (approximately 3 nm in thickness) can also be seen surrounding the islands. This oxide layer is expected to have grown after the samples were removed from the deposition system. Following oxidation at 600 ºC, the discrete cores and oxide shells were no longer visible and the microstructure of the SnO_x clusters became more complex, containing small crystallites and voids. Selected area diffraction patterns from the as-deposited and *Ox600* sample (not shown) could be indexed to metallic Sn and rutile SnO_2, respectively. No evidence could be found for metallic Sn reflections in the diffraction pattern from the *Ox600* sample indicating that the Sn clusters had fully transformed into SnO_2 following oxidation to 600 ºC.

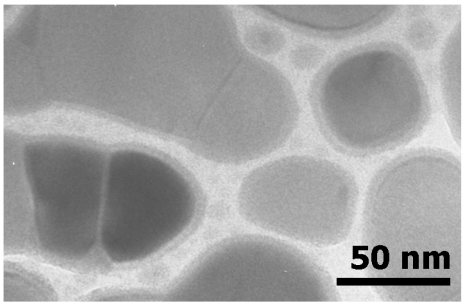

(a)

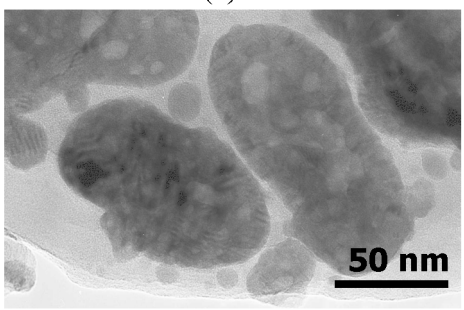

(b)

Figure 4. Plan view TEM images of evaporated Sn clusters (a) as-deposited and (b) after oxidation at temperatures of 200 ºC, 400 ºC and 600ºC.

The changes in morphology and structure of the islands which occur due to the annealing process are seen in more detail in the cross-sectional TEM (X-TEM) images shown in Fig. 5. The discrete core and shell structure of the as-deposited islands (Fig. 5(a) – sample *AsDep*) was again clearly evident, and grew thicker (from ~ 3 nm to ~ 8 nm) after oxidation at 200 ºC (Fig. 5(b) – sample *Ox200*). A thin SnO_x layer can also be seen at the island-surface interface which is believed to have formed due to the presence of water vapour on the sample surface during the thermal evaporation process. Using additional X-TEM images of the islands on the *Ox200* sample, it was found that in smaller islands (with lengths less than ~20 nm) the oxide shells always occupied more than 50 % of the island's cross-sectional area. Once oxidised, these islands become less mobile and less able to coalesce, which explains the population of small islands (with areas less than 2000 nm^2) observed on samples *Ox400* and *Ox600*. X-TEM images of the samples *Ox400* and *Ox600* are shown in Figs. 5(c) and 5(d), respectively. The Sn cores are no longer visible and the

perpendicular height to length ratio has clearly changed as a result of the higher temperatures experienced by these samples. The *Ox600* sample was obviously polycrystalline and the crystallites in the cross-sectioned *Ox600* clusters had areas of between 5 nm^2 and 500 nm^2.

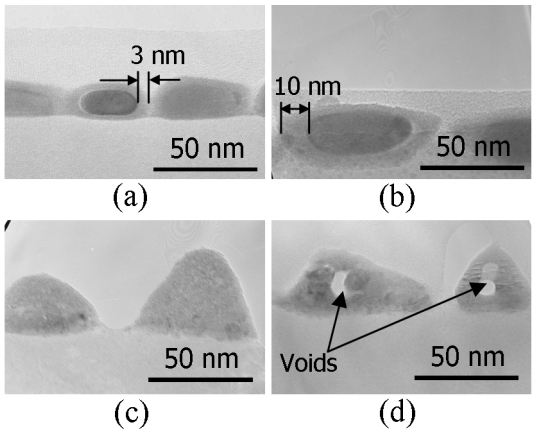

Figure 5. X-TEM images of $Sn/SnO_x/SnO_2$ clusters (a) as-deposited, (b) after oxidation at 200 ºC, (c) after oxidation at temperatures of 200 ºC and 400 ºC and (d) after oxidation at temperatures of 200 ºC, 400 ºC and 600 ºC.

The contact angle for the as-deposited Sn islands is typically greater than 120º. The islands therefore exhibit a low thermodynamic work of adhesion ($W_{ad} < 0.4$ J m^{-2}) according to the Young–Dupre equation [19],

$$W_{ad} = \gamma_m (1 + \cos \theta), \quad (1)$$

where γ_m is the surface energy of the metal, θ is the contact angle and W_{ad} is the work of adhesion. This is consistent with the expected wetting behaviour for low melting point metal islands supported on a metal or silicon oxide. Following annealing, the contact angle of the oxidised islands becomes sub-90º as they change into a mould like shape. This change in morphology can be attributed to two competing mechanisms. Firstly, the island is 'anchored' to the substrate due to the strength of the bond between the interfacial oxide and the underlying SiO_2. Secondly, as the temperature exceeds 230 ºC and the Sn core

becomes molten, it adopts an energetically favourable sphere-like shape. The surface oxide conforms to the sphere-like core except at the island-substrate interface where it remains firmly adhered as the energy of attachment is high for an oxide-oxide interface. The contact angle of the island therefore reduces as a result of the oxidation process. As the perpendicular height of the fully oxidised islands is significantly greater than that of the as-deposited islands, the volume of the islands has increased. The average volumetric change was estimated from the TEM and SEM images to be more than 50 %. Thermally assisted coalescence of neighbouring clusters and the formation of pores, which were clearly visible in the clusters of the *Ox600* sample, were responsible for the larger than expected volume increase. One explanation for the occurrence of these voids may be that if the temperature exceeds 400 ºC, any remaining Sn out-gasses sufficiently to create 'bubbles' which cannot escape through the surrounding oxide. Alternatively, they may be caused simply by thermal expansion and contraction of Sn and/or SnO_x within the clusters occurring as a result of the RGTO process. Some densification of the SnO_2 is expected to occur due to crystallisation at temperatures between 400 ºC and 600 ºC but it is unlikely that this effect alone is capable of producing voids as large as those seen in the *Ox600* sample.

3.4. Gas sensing measurements

The attributes of the SnO_2 film which was oxidised at temperatures up to 600 ºC (high surface-area, nanoscale clusters and pores) suggested that it may be capable of gas sensing. A prototype sensor was therefore fabricated and tested. Fig. 6(a) shows a SEM image of a RGTO treated SnO_2 cluster film supported on dual inter-digital eletrodes and a passivated Si substrate. As mentioned previously, this film was produced using two evaporations with RGTO processes following each of the evaporations. TEM inspection of a small section of the film revealed that the clusters were polycrystalline with similar nanostructure to that shown in Fig. 5(d). The sensor film clearly has high surface area and appears coral-like in its morphology (as seen in Fig. 6(a)). Neighbouring clusters are more densely packed in this thicker film than they are in the films shown in Fig. 1 and the probability of coalescence is therefore higher.

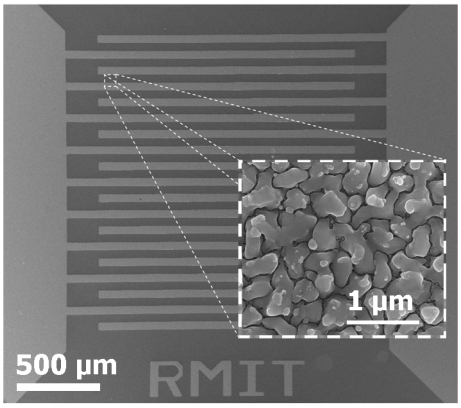

(a)

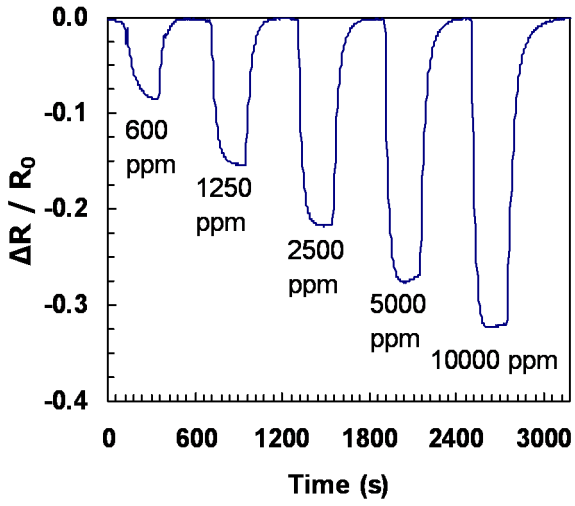

(b)

Figure 6. (a) A SnO_2 thin-film deposited on Au interdigital electrodes and (b) the normalised resistance change exhibited by the film when exposed to different concentrations of hydrogen gas (as marked in ppm) and operating at a temperature of 150 ºC.

Fig. 6(b) shows the normalised change in resistance ($\Delta R/R_0$, where R_0 is the resistance with zero exposure) caused by pulsed hydrogen exposures of concentrations 625 ppm, 1250 ppm, 2500 ppm, 5000 ppm and 10000 ppm at a temperature of 150 ºC. With a H_2 gas concentration of 2500 ppm, the response and recovery times for the sensor were 50 s and 70 s, respectively. NO_2 gas sensing tests were also performed and upon exposure to a concentration of NO_2 gas of 500 ppb, the resistance of the film increased from

8.4 kΩ to 18.9 kΩ. The response and recovery times exhibited for this concentration of NO_2 were 50 s and 90 s, respectively. These results compare favourably with previous results for undoped SnO_2 thin-film sensors [4]. We are now planning to use the prototype sensor and TEM to assess whether the structure of the porous polycrystalline SnO_2 film remains stable after long term exposure to NO_2 and H_2.

4. Summary

The RGTO technique was used to prepare SnO_x clusters from discontinuous evaporated Sn thin films. Samples with different ultimate oxidation temperatures were characterised and the stoichiometry, morphology and micro-structure determined. Selected area diffraction patterns and TEM images showed that the as-deposited Sn clusters were polycrystalline with a ~ 3 nm thick native oxide layer and a well defined inner Sn core. The remaining samples showed that the oxide layer grows to ~ 8 nm thickness after oxidation for 2-hrs at 200 ºC and the metallic Sn core was no longer evident when the maximum oxidation temperature was 400 ºC or 600 ºC. XPS and selected area diffraction showed that the clusters oxidised up to 600 ºC were substantially SnO_2, as previously reported and that they were polycrystalline. Crystallites with cross-sectional areas of between 5 nm^2 and 500 nm^2 were seen in these clusters. Whilst the morphology of the SnO_2 cluster film was not dramatically different from the as-deposited Sn cluster film, the average volume of the SnO_2 clusters was significantly larger. Voids were found in many of the SnO_2 clusters and undoubtedly contributed to the observed increase in volume. Finally, a prototype sensor based on RGTO processed thermally evaporated Sn was tested and found to exhibit good sensitivity to H_2 and NO_2 gases making them suitable for many commercial applications.

REFERENCES

[1] Ihokura K and Watson J 1994 The Stannic Oxide Gas Sensor: Principles and Applications (Florida: CRC Press)

[2] Schierbaum K D, Weimar U and Goepel W 1992 *Sensors and Actuators* B **7** 709

[3] Kalantar-zadeh K and Fry B 2007 *Nanotechnology-Enabled Sensors* (New York: Springer)

[4] Lou X, Peng C, Wang X and Chu W 2007 *Vacuum* **81** 883

[5] Shanthi E, Dutta V, Banerjee A and Chopra K L 1980 *J. Appl. Phys.* **51** 6243

[6] Dattoli E N, Wan Q, Guo W, Chen Y, Pan X and Lu W 2007 *Nano Letters* **7** 2463

[7] El Khakani M A, Dolbec R, Serventi A M, Horrillo M C, Trudeau M, Saint-Jacques R G, Rickerby D G and Sayago I 2001 *Sensors and Actuators* B **77** 383

[8] Pan X Q and Fu L 2001 *Journal Applied Physics* **89** 6048

[9] Micocci G, Tepore A, Serra A, Siciliano P and Ali-Adib Z 1996 *Vacuum* **47** 1175

[10] G Sberveglieri G, G Faglia G, S Groppelli S, P Nelli P and Camanzi A 1990 *Semiconductor Science and Technology* **5** 1231

[11] Kolmakov A, Zhang Y and Moskovits M 2003 *Nano Letters* **3** 1125

[12] Geurts J, Rau S, Richter W and Schmitte F J 1984 *Thin Solid Films* **121** 217

[13] Park G-S and Yang G-M 2000 *Thin Solid Films* **365** 7

[14] Nelli P, Faglia G, Sberveglieria G, Ceredab E, Gabettab G, Dieguezc A, Romano-Rodriguezc A and Morante J R 2000 *Thin Solid Films* **371** 249

[15] Aste T, Botter R and Beruto D 1995 *Sensors and Actuators* B **24** 826

[16] Sigma Aldrich SnO2 Prod. no. 244651-100G 99.9% -325 mesh

[17] Ostwald W 1900 *Z. Phys. Chem.* **34** 495

[18] Briggs D and Seah M P (Ed.) 1990 *Practical Surface Analysis* 2nd edition Vol. 1 *Auger and Xray Photoelectron Spectroscopy* (England: Wiley) p. 642

[19] Howe J M 1997 *Interfaces in Materials* (New York: Wiley) p. 182